

## Large Low-Field Magnetoresistance in Perovskite-type $\text{CaCu}_3\text{Mn}_4\text{O}_{12}$ without Double Exchange

Z. Zeng and M. Greenblatt\*

*Department of Chemistry, Rutgers, the State University of New Jersey, Piscataway, New Jersey 08854-8087*

M. A. Subramanian

*Dupont Central Research and Development, Wilmington, Delaware 19880-0328*

M. Croft

*Department of Physics, Rutgers, the State University of New Jersey, Piscataway, New Jersey 08854-8019*

(Received 5 October 1998)

We report the observation of large low-field magnetoresistance (MR) behavior in  $\text{CaCu}_3\text{Mn}_4\text{O}_{12}$  with a perovskite-related ( $AA'_3B_4O_{12}$ ) structure.  $\text{Ca}^{2+}\text{Cu}^{2+}_3\text{Mn}^{4+}_4\text{O}_{12}$  is semiconducting and orders ferromagnetically at 355 K. However, it has neither mixed valency of Mn for double-exchange magnetic interactions, nor Jahn-Teller  $\text{Mn}^{3+}$  ions, nor a metal-insulator transition. The MR smoothly increases with decreasing temperature and is  $-40\%$  at 20 K. The low-field MR response does not show the strong temperature-dependent decay characteristic of the  $\text{LnMnO}_3$  perovskite-based systems and appears consistent with an intergrain-interdomain tunneling origin. [S0031-9007(99)08905-X]

PACS numbers: 75.50.Dd

A common property of the alkaline earth (A) substituted rare earth manganates,  $\text{Ln}_{1-x}\text{A}_x\text{MnO}_3$  is a semiconductor-to-metal transition near a paramagnetic-to-ferromagnetic transition, the Curie temperature ( $T_C$ ) [1–3]. In general, the highest magnetoresistance [ $\text{MR} = (\rho_H - \rho_0)/\rho_0$ , where  $\rho_H$  and  $\rho_0$  are the resistivities at applied magnetic fields of  $H$  and 0, respectively] is observed close to the semiconductor-to-metal transition temperature ( $T_{IM}$ ). It is considered that in the rare earth perovskites the CMR originates from an applied magnetic field enhanced spin-charge-coupled magnetotransport phenomena. In  $\text{Ln}_{1-x}\text{A}_x\text{MnO}_3$ , A ion substitution for Ln produces  $\text{Mn}^{4+}$  ions with itinerant  $e_g$  holes which overlap with O  $2p$  orbitals. The double-exchange (DE) [4] interaction between  $\text{Mn}^{3+}\text{-O-Mn}^{4+}$  mediates charge transfer and ferromagnetic interaction, and below the Curie temperature,  $T_C$ , the sample is metallic (i.e.,  $T_{IM} \approx T_C$ ). Near  $T_C$  the applied magnetic field tends to align the local spins, which enhances electron transfer and leads to a dramatic decrease in the observed resistivity.

Because the MR of the colossal magnetoresistance (CMR) materials can be very large,  $\sim 100\%$ , these materials have potential applications for magnetic memory and actuator devices. However, before practical applications can be realized critical properties of the CMR materials must be improved. For example, the MR values are high at the  $T_C/T_{IM}$  transition and at high  $H$  (several tesla), but the response at low field and at room temperature is negligible. Although much effort has been made to improve the MR response of the manganates, the MR at room temperature and low fields is significantly lower than that of the conventional giant magnetoresistance (GMR) materials [2,5]. Further, the MR effect of the manganates is sharply peaked near  $T \approx T_C/T_{IM}$ , thereby yielding a nar-

row temperature range of stable high MR. For practical application, significant temperature stability is required.

The recent report of the pyrochlore  $\text{Tl}^{3+}_2\text{Mn}^{4+}_2\text{O}_7$  compound represented a novel extension of the CMR materials both by virtue of the absence of  $\text{Mn}^{3+}\text{-O-Mn}^{4+}$  DE and of its departure from the perovskite structure [6,7]. Here we report the observation of a large MR for the first time in a perovskitelike manganate,  $\text{CaCu}_3\text{Mn}_4\text{O}_{12}$  with only  $\text{Mn}^{4+}\text{-O-Mn}^{4+}$  interactions at the B site, hence without the possibility of DE operating. Moreover, both the magnitude and thermal stability of this MR are shown to be of potential technological utility.

$\text{CaCu}_3\text{Mn}_4\text{O}_{12}$  was investigated by Chenavas *et al.* and Bochu *et al.* [8,9]. Single crystal X-ray structural analysis showed that  $\text{ACu}_3\text{Mn}_4\text{O}_{12}$  crystallizes in a perovskite-like phase ( $AA'_3B_4O_{12}$ ) with cubic symmetry (space group  $Im\bar{3}$ ) with a doubling of the ideal perovskite cell. The doubling of the unit cell is due to the ordering of the  $\text{Ca}^{2+}$  and  $\text{Cu}^{2+}$  ions and the distortion of the oxygen sublattice which leads to a tilted three-dimensional network of  $\text{MnO}_6$  octahedra sharing corners (Fig. 1). The Mn-O-Mn bond angle is  $\sim 142^\circ$  instead of  $180^\circ$ , as in the ideal perovskite structure. This distortion creates two different polyhedra at the A site: a slightly distorted 12 oxygen-coordinated cubooctahedral Ca (A) site and a grossly distorted icosahedron at the Cu (A') site. There are three sets of Cu-O distances at  $\sim 1.9$ ,  $2.8$ , and  $3.2$  Å, each forming an approximately square-planar coordination. The unusual feature of this structure is that it requires a Jahn-Teller ion, such as  $\text{Cu}^{2+}$  (or  $\text{Mn}^{3+}$ ), at the A' site [9].

$\text{CaCu}_3\text{Mn}_4\text{O}_{12}$  was prepared from a stoichiometric mixture of high purity  $\text{Ca(OH)}_2$ ,  $\text{CuO}$ , and  $\text{MnO}_2$  mixed with 15%  $\text{KClO}_3$ . The mixture was sintered at  $1000^\circ\text{C}$  and 58 kbar for 30 min. The product was ground to a

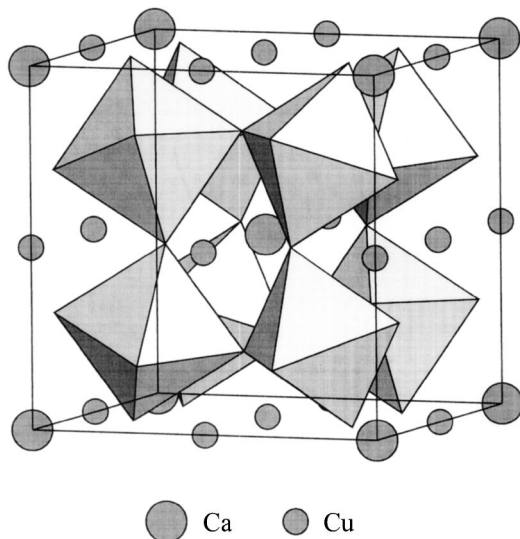


FIG. 1. Structure of  $\text{CaCu}_3\text{Mn}_4\text{O}_{12}$  indicating the  $\text{MnO}_6$  polyhedral structure. The cubooctahedral  $\text{CaO}_{12}$  and the highly distorted 12-coordinated polyhedra around the  $\text{Cu}^{2+}$  fill alternate cavities created by the three-dimensional network of corner-sharing  $\text{MnO}_6$  octahedra.

finite powder and washed several times with deionized water under ultrasonic conditions to dissolve KCl. The powder x-ray diffraction (SCINTAG PAD V,  $\text{CuK}_\alpha$ ) indicated formation of single phase  $\text{CaCu}_3\text{Mn}_4\text{O}_{12}$  with cubic symmetry (space group  $Im\bar{3}$ ) and a unit cell with  $a = 7.21348(4)$  Å in good agreement with previous results [8,9]. Chemical analysis [inductively coupled plasma emission spectrometer (ICP); Baird Atomic Model 2070] shows that Ca:Cu:Mn is 1:2.97:4.02 in excellent agreement, within the experimental error (2%), with the expected values for  $\text{CaCu}_3\text{Mn}_4\text{O}_{12}$ . The oxidation state of Mn is 3.99, as determined by dissolving a sample of  $\text{CaCu}_3\text{Mn}_4\text{O}_{12}$  in dilute sulfuric and phosphoric acid with an excess of  $\text{Fe}(\text{NH}_4)_2(\text{SO}_4)_2$  and titrating with a standard solution of  $\text{KMnO}_4$ .

Since the  $\text{Mn}^{4+}$  character of this material is central to its novelty, the oxidation states of Mn and Cu in  $\text{CaCu}_3\text{Mn}_4\text{O}_{12}$  were also investigated by x-ray absorption near-edge spectroscopy (XAS) to establish this point. The Mn and Cu K-edge XAS measurements were performed on beam lines X-19A and X-18B at the Brookhaven National Synchrotron Light Source using a double crystal Si(311) and channel-cut Si(111) monochromator, respectively. A standard was run simultaneously with all measurements for precise calibration. All spectra were normalized to unity step in the absorption coefficient.

The Mn-K main edge of  $\text{CaCu}_3\text{Mn}_4\text{O}_{12}$  is compared to those of standard  $\text{Mn}^{3+}$  and  $\text{Mn}^{4+}$  standards in Fig. 2. Although the detailed shape of such Mn-K edge spectra can vary between different compounds, the shift to higher energies of the higher valent spectra (typical to all core level spectroscopies) can be still discerned. This shift is clearest between the La ( $\text{Mn}^{3+}$ ) and Ca ( $\text{Mn}^{4+}$ ) perovskite spectra. Although the  $\text{Mn}^{4+}$ - $\text{MnO}_2$  spectrum

exhibits features that are split up and down in energy, the edge centum, near the absorption coefficient  $\mu = 0.8$  coincides very well with the steeply rising portion of the  $\text{Mn}^{4+}$ - $\text{CaMnO}_3$  spectrum. The shift of  $\text{CaCu}_3\text{Mn}_4\text{O}_{12}$  edge strongly supports the  $\text{Mn}^{4+}$  assignment for this compound in agreement with that (3.99) obtained by chemical titration.

The pre-edge  $a$  feature in Fig. 2 is associated with transitions into  $d/d-p$ -hybridized final states; and has been shown to increase in strength with increasing Mn valence (or  $d$ -hole population) [10]. In the inset of Fig. 2 an expanded view of this  $a$  feature clearly manifests a spectral intensity comparable to the  $\text{Mn}^{4+}$  standards and far greater than the  $\text{Mn}^{3+}$  standard. The  $a1$ - $a2$  subfeature splitting and intensity ratio, typical of the  $\text{Mn}^{4+}$  state spectra (see inset), are also replicated in the  $\text{CaCu}_3\text{Mn}_4\text{O}_{12}$   $a$ -feature. Such  $a1$ - $a2$  feature splittings have been attributed in the past to the  $3d t_{2g}$ - $e_g$  splitting [11]. The particularly high resolution of these spectra also allows the identification of a third  $a3$  subfeature common to both the  $\text{CaMnO}_3$  and  $\text{CaCu}_3\text{Mn}_4\text{O}_{12}$  spectra. Thus the strength and structure of the Mn preedge further reinforce the  $\text{Mn}^{4+}$  assignment in this material. The Cu K edge XAS (not shown) indicated unambiguously that the formal valence of Cu is 2+ in this and a related class of materials with Mn substituted at the Cu sites [12].

The dc electrical resistivity ( $\rho$ ) and MR measurements were carried out using a conventional four-probe technique. The resistivity samples were pressed under 15 kbar of pressure. Gold leads were attached to the sample with baked silver paste. The magnetoresistance and magnetic measurements were carried out from 20 to 400 K in a SQUID magnetometer (MPMS, Quantum Design).

The temperature dependence of the low-field magnetization of  $\text{CaCu}_3\text{Mn}_4\text{O}_{12}$  in Fig. 3A shows a ferromagnetic transition near 355 K. The coercivity ( $H_c$ ) is only

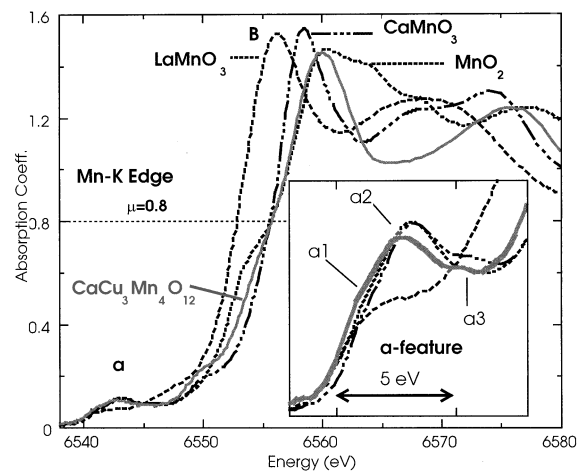


FIG. 2. The Mn K edges of  $\text{CaCu}_3\text{Mn}_4\text{O}_{12}$ , along with those of the  $\text{Mn}^{3+}$ - $\text{LaMnO}_3$ ; and the  $\text{Mn}^{4+}$ - $\text{CaMnO}_3$  and  $\text{Mn}^{4+}$ - $\text{MnO}_2$  standards. The inset is an expanded view of the pre-edge  $a$  features of these spectra.

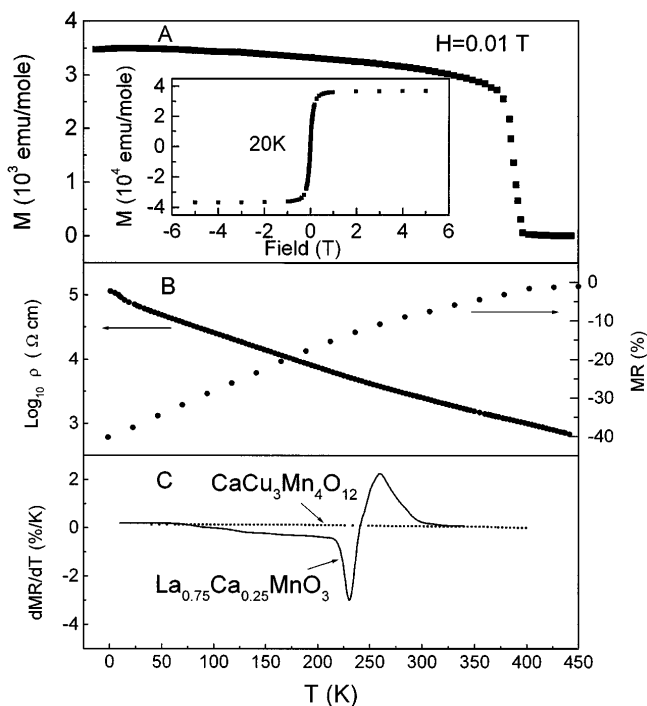


FIG. 3. Magnetization as a function of temperature for  $\text{CaCu}_3\text{Mn}_4\text{O}_{12}$  (A). Resistivity and MR% ( $H = 0$  and  $5$  T) as a function of temperature (B).  $d(\text{MR})/dT$  as a function of temperature at  $5$  T (C).

$70$  G at  $20$  K, and  $10$  G at  $300$  K (see Fig. 3A-inset) indicating that  $\text{CaCu}_3\text{Mn}_4\text{O}_{12}$  is a soft ferromagnetic material. Recall that the  $\text{Mn}^{4+}$ -pyrochlore,  $\text{Tl}_2\text{Mn}_2\text{O}_7$  manifests a coupled insulator-to-metal and paramagnetic-to-ferromagnetic transitions [6,7].  $\text{CaCu}_3\text{Mn}_4\text{O}_{12}$  provides an example of a perovskite-type structure with Mn only in the  $4+$  oxidation state with ferromagnetic ordering. It is well established that the Mn-O-Mn bond angle is a critical factor in determining the nature of the magnetic interactions in manganates.  $\text{Mn}^{4+}$ -O- $\text{Mn}^{4+}$  ( $d^3$ )  $180^\circ$  superexchange interactions generally lead to antiferromagnetic ordering while  $90^\circ$  superexchange will result in ferromagnetic ordering [13]. It was suggested that the ferromagnetism of  $\text{Tl}_2\text{Mn}_2\text{O}_7$  is due to superexchange interactions, as the Mn-O-Mn bond angle of  $134^\circ$  is intermediate between  $90^\circ$  and  $180^\circ$  [7]. The Mn-O-Mn bond angle in  $\text{CaCu}_3\text{Mn}_4\text{O}_{12}$  is  $142^\circ$ , therefore, the observed ferromagnetic transition similarly may be related to superexchange interactions. However, the magnetic interactions in  $\text{CaCu}_3\text{Mn}_4\text{O}_{12}$  are more complex than those in  $\text{Tl}_2\text{Mn}_2\text{O}_7$  involving the heteromagnetic ions,  $\text{Mn}^{4+}$  and  $\text{Cu}^{2+}$  arranged in alternate sites of the perovskite lattice. Thus the competing coupling between the magnetic  $A'$ -site  $\text{Cu}^{2+}/\text{Cu}^{2+}$  and  $B$ -site  $\text{Mn}^{4+}/\text{Mn}^{4+}$  ions may influence its properties also.

Qualitative Seebeck measurement of  $\text{CaCu}_3\text{Mn}_4\text{O}_{12}$  indicates  $n$ -type behavior. The  $\log_{10}\rho$  as a function of temperature in Fig. 3B shows that  $\text{CaCu}_3\text{Mn}_4\text{O}_{12}$  is semiconducting between  $20$ – $300$  K with a room temperature resistivity ( $\rho_{\text{RT}}$ ) of  $\sim 1.8 \times 10^3 \Omega \text{ cm}$ . The plot of

$\log_{10}\rho$  vs  $1/T$  (see Fig. 4) indicates a temperature dependence more complex than simple activation. Although there is a change in the effective activation energies from above to below  $T_C$  the limited temperature region above  $T_C$  makes definitive conclusions difficult. There is no clear critical anomaly in the vicinity of  $T_C$  either in the resistivity or its derivative.

The magnetoresistance of  $\text{CaCu}_3\text{Mn}_4\text{O}_{12}$  is  $-40.3\%$  at  $20$  K and  $5$  T (Fig. 3B). It is evident in Fig. 3C that the temperature stability of the MR of  $\text{CaCu}_3\text{Mn}_4\text{O}_{12}$  is superior to that of  $\text{La}_{0.75}\text{Ca}_{0.25}\text{MnO}_3$ , a typical CMR manganate.

As indicated above, the large MR in  $\text{CaCu}_3\text{Mn}_4\text{O}_{12}$  is not likely due to DE mechanism. Moreover, we also prepared  $\text{CaCu}_{2.5}\text{Mn}_{4.5}\text{O}_{12}$  [ $\text{Ca}(\text{Cu}^{2+}_{2.5}\text{Mn}^{3+}_{0.5})(\text{Mn}^{3+}_{0.5}\text{Mn}^{4+}_{3.5})\text{O}_{12}$ ] and  $\text{CaCu}_2\text{Mn}_5\text{O}_{12}$  [ $\text{Ca}(\text{Cu}^{2+}_2\text{Mn}^{3+})(\text{Mn}^{3+}\text{Mn}^{4+}_3)\text{O}_{12}$ ] with mixed valent  $\text{Mn}^{3+/4+}$  on the  $B$  site and the possibility of  $\text{Mn}^{3+}$ -O- $\text{Mn}^{4+}$  DE mechanism operating [12]. However, the MR of these compounds is significantly smaller than that of  $\text{CaCu}_3\text{Mn}_4\text{O}_{12}$ . Thus it is concluded that in the  $\text{CaCu}_{3-x}\text{Mn}_{4+x}\text{O}_{12}$  system the MR is not due to the DE mechanism.

Figure 4A shows the MR as a function of  $H$  at  $20$  K. The MR sharply increases at low fields, and almost saturates at  $\sim 1$  T. The MR is  $-12\%$  at  $0.05$  T.  $\text{La}_{0.6}\text{Y}_{0.07}\text{Ca}_{0.33}\text{MnO}_3$  was reported to have a CMR,  $\sim 100\%$  at high fields, but the MR is only  $6.5\%$  at  $0.05$  T [3]. In other systems, such as  $\text{La}(B)\text{CoO}_3$  [14], Cr-based chalcogenide [15], and  $\text{Tl}_2\text{Mn}_2\text{O}_7$  [6,7] the low-field MR is also very low. Figure 4B compares  $\text{MR}_H/\text{MR}_{5T}$  (where  $\text{MR}_H$  and  $\text{MR}_{5T}$  are the MR at  $H$  and  $5$  T, respectively) as a function of  $H$  in several systems [3,6,14,15]. At low fields,  $\text{CaCu}_3\text{Mn}_4\text{O}_{12}$  exhibits a much sharper response than any of the other systems. The MR as a function of field at  $300$  K is shown in Fig. 4A, inset. In contrast to the MR at  $20$  K, the MR at room temperature is almost saturated at only

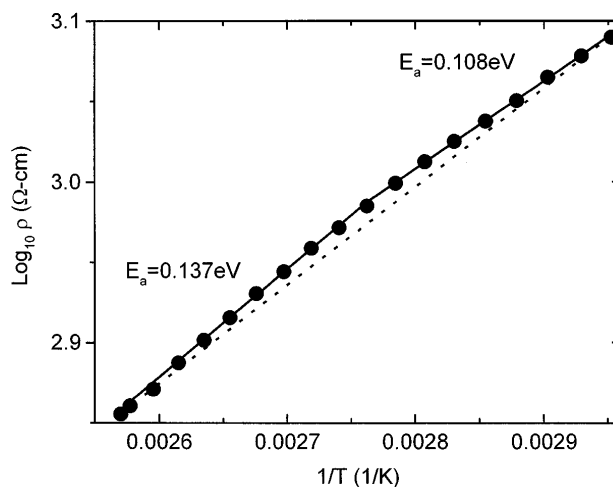


FIG. 4. The variation of  $\log_{10}\rho$  as a function of  $1/T$  for  $\text{CaCu}_3\text{Mn}_4\text{O}_{12}$ .

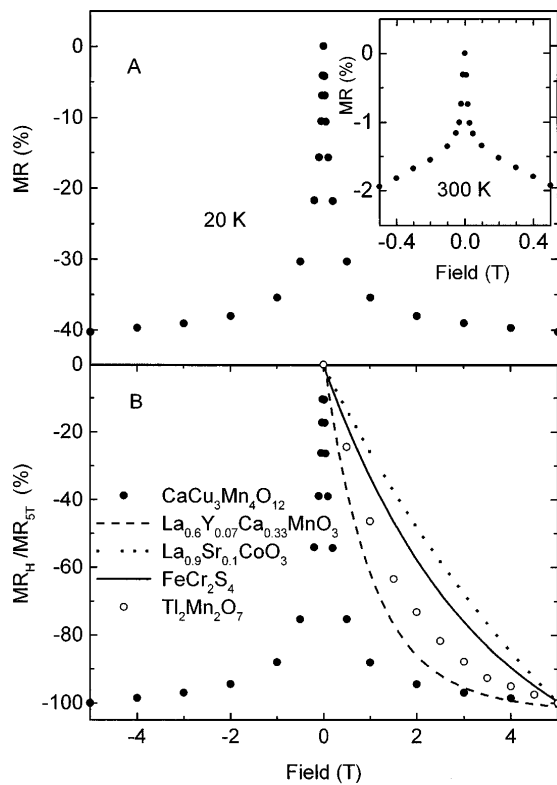


FIG. 5. MR as a function of  $H$  for  $\text{CaCu}_3\text{Mn}_4\text{O}_{12}$  at 20 and 300 K (A).  $\text{MR}_H/\text{MR}_{5T}$  as a function of  $H$  for  $\text{CaCu}_3\text{Mn}_4\text{O}_{12}$ ,  $\text{La}_{0.6}\text{Y}_{0.07}\text{Ca}_{0.33}\text{MnO}_3$ ,  $\text{La}_{0.9}\text{Sr}_{0.1}\text{CoO}_3$ ,  $\text{FeCr}_2\text{S}_4$ , and  $\text{Ti}_2\text{Mn}_2\text{O}_7$  (B).

0.03 T. At low fields and room temperature, the MR sharply responds to  $H$ . The  $\rho_{RT}$  of  $\text{CaCu}_3\text{Mn}_4\text{O}_{12}$  ( $1.8 \times 10^3 \Omega \text{ cm}$ ) is 8 orders of magnitude higher than that of permalloy, 80Ni-20Fe ( $10^{-5} \Omega \text{ cm}$ ) [16]. If we define  $\rho_0 \times \text{MR}$  as a relative output voltage,  $\rho_0 \times \text{MR}$  of  $\text{CaCu}_3\text{Mn}_4\text{O}_{12}$  is  $\sim 10^6$  higher than that of permalloy at 10 G and room temperature. This behavior is promising for potential application of  $\text{CaCu}_3\text{Mn}_4\text{O}_{12}$  as a magnetic sensor material.

Thus, by virtue of its  $\text{Mn}^{4+}$  character,  $\text{CaCu}_3\text{Mn}_4\text{O}_{12}$  represents the first perovskitelike, large-MR material for which double exchange is precluded from driving the ferromagnetic (FM) exchange or MR. Moreover, it is also the first of this perovskite-based class of materials to lack a magnetically coupled IM transition. Regarding the MR mechanism in this material, the similar saturation fields in the FM-domain reorientation (the coercive field) and in the MR suggests an interdomain/grain tunneling mechanism origin for the MR [5]. The relatively smooth vanishing of the thermal variation of the MR near  $T_C$  would be consistent with the coupling of the MR (to first order) to the square of the magnetization order param-

eter [5]. Additional enhancement of the MR at low temperatures would be anticipated from the freezing out of phonon and domain-wall-impurity assisted tunneling as well as from localization effects. Future work on these issues and on the role of the Cu sublattice magnetic moments on both the magnetism and transport are clearly called for.

We thank Professor K. V. Ramanujachary for his suggestions with experimental problems and useful discussions. The ICP analysis was carried out in the Chemistry Department of Rider College with the help of Dr. W. H. McCarroll. This work was supported by National Science Foundation-Solid State Chemistry Grant No. DMR-96-13106.

\*To whom correspondence should be addressed.

- [1] S. Jin, T. H. Tile, M. McCormack, R. A. Fastnacht, R. A. Ramesh, and L. H. Chen, *Science* **264**, 413 (1994).
- [2] X. L. Wang, S. X. Dou, H. K. Liu, M. Lonescu, and B. Zeimetz, *Appl. Phys. Lett.* **73**, 396 (1998).
- [3] S. Jin, H. M. O'Bryan, T. H. Tiefel, M. McCormack, and W. W. Rhodes, *Appl. Phys. Lett.* **66**, 382 (1995).
- [4] C. Zener, *Phys. Rev.* **82**, 403 (1951).
- [5] H. Y. Hwang, S-W. Cheong, N. P. Ong, and B. Batlogg, *Phys. Rev. Lett.* **77**, 2041 (1996).
- [6] Y. Shimakawa, Y. Kubo, and T. Manako, *Nature (London)* **379**, 53 (1996).
- [7] M. A. Subramanian, B. H. Toby, A. P. Ramirez, W. J. Marshall, A. W. Sleight, and G. H. Kwei, *Science* **273**, 81 (1996).
- [8] J. Chenavas, J. C. Joubert, M. Marezio, and B. Bochu, *J. Solid State Chem.* **14**, 25 (1975).
- [9] B. Bochu, J. C. Joubert, A. Collomb, B. Ferrand, and D. Samaras, *J. Magn. Magn. Mater.* **15**, 1319 (1980).
- [10] M. Croft, D. Sills, M. Greenblatt, C. Lee, S-W. Cheong, K. V. Ramanujachary, and D. Tran, *Phys. Rev. B* **55**, 8726 (1997).
- [11] A. Shainer, M. Croft, Z. Zhang, M. Greenblatt, I. Perez, P. Metcalf, H. Jhans, G. Liang, and Y. Jeon, *Phys. Rev. B* **53**, 9745 (1996).
- [12] Z. Zeng, J. Sunstrom IV, M. Greenblatt, and M. Croft, *J. Solid State Chem.* (to be published).
- [13] J. B. Goodenough, *Magnetism and the Chemical Bond* (Interscience Publishers, New York, 1963).
- [14] R. Mahendiran, A. K. Raychaudhuri, A. Chainani, and D. D. Sarma, *J. Phys. Condens. Mater.* **7**, L561 (1995).
- [15] A. P. Ramirez, R. J. Cava, and J. Krajewski, *Nature (London)* **386**, 156 (1997).
- [16] *Ferromagnetic Materials*, edited by E. P. Wohlfarth (North-Holland Publishing Company, Amsterdam, 1980), Vol. 2, p. 66.